Journal of Minerals and Materials Characterization and Engineering, 2018, 6, 373-381
http://www.scirp.org/journal/jmmce
ISSN Online: 2327-4085
ISSN Print: 2327-4077

The High Surface Ratio Micro-MoS_2 Grain Composed of MoS_2 Nanosheet Prepared with One-Step Hydrothermal Synthesis

Guangtong Zhou[1], Xiangbin Zeng[2*], Wenzhao Wang[2], Yishuo Hu[2], Sue Xu[1], Shaoxiong Wu[2], Yang Zeng[2], Wen Jing[1], Tingting Ren[2], Zhenyu Guo[2], Pengfei Xu[2], Haoran Li[2], Yushu Tang[2]

[1]China-EU Institute for Clean and Renewable Energy, Huazhong University of Science and Technology, Wuhan, China
[2]School of Optical and Electronic Information, Huazhong University of Science and Technology, Wuhan, China
Email: *eexbzeng@163.com

How to cite this paper: Zhou, G.T., Zeng, X.B., Wang, W.Z., Hu, Y.S., Xu, S., Wu, S.X., Zeng, Y., Jing, W., Ren, T.T., Guo, Z.Y., Xu, P.F., Li, H.R. and Tang, Y.S. (2018) The High Surface Ratio Micro-MoS_2 Grain Composed of MoS_2 Nanosheet Prepared with One-Step Hydrothermal Synthesis. *Journal of Minerals and Materials Characterization and Engineering*, **6**, 373-381.
https://doi.org/10.4236/jmmce.2018.63026

Received: March 29, 2018
Accepted: May 14, 2018
Published: May 17, 2018

Abstract

Micro molybdenum disulfide was prepared with one-step hydrothermal method; the influence of reactant concentration and temperature on the surface ratio of micro-MoS_2 grain was investigated. Raman spectroscopy (Raman), X-ray diffraction (XRD), and Scanning electron microscopy (SEM) were used to characterize the structure, composition and morphology of MoS_2. The results show that micro-MoS_2 grains were synthesized with one-step hydrothermal synthesis, and the morphology of micro-MoS_2 grains is like flower and sphere. The SEM figures indicate that the surface ratio of micro-MoS_2 grains is different and also show that the surface ratio of micro-MoS_2 grains can be improved by regulating reactant concentration and temperature. This research showed a method to improve the surface ratio of micro-MoS_2 grains.

Keywords

Micro-MoS_2 Grain, Hydrothermal, One-Step Reaction, Nanosheet

1. Introduction

The transition metal dichalcogenide (TMDC) attracted great attention due to their excellent chemical, electrical and optical properties over the past decade [1] [2] [3]. Graphene was the first 2D material to be found [4] [5]. Graphene has very high carrier mobility, strength, surface area and thermal conduction capability [6] [7] [8] [9] [10], so graphene has great potential applicant in many fields. But graphene's band gap is zero, limiting its electronic applications. Molybdenum disulfide (MoS_2) is the most studied TMDC, which has a special mi-

crostructure like sandwich (S-Mo-S), Mo-layer between two sulfur layers by covalent forces, and is relatively abundant as a mineral and well-known for tribological, petroleum desulfurization and catalytic applications [11].

Because of its high surface ratio, micro-size MoS_2 plays a crucial role in battery cathodes domain [12]. The devices of energy-storage play an important role in reducing the emission of greenhouse gas, wasting of resources and the environmental pollution [13] [14] [15] [16] [17]. MoS_2 could be used in these devices of energy-storage. L. X. Chen etc. improved the capacity retention rate of the composite electrode up to 50.5% at the current density of 3000 mAg^{-1} when discharging through coating MoS_2 on the surface of hydrogen storage alloys [18].

The gas molecules can infiltrate and diffuse freely between the vertically stacked S-Mo-S layers. After the adsorption and diffusion of gas molecules between the S-Mo-S layers, the resistance of MoS_2 will change prominently; because of that tremendous research has been made in gas sensing application, such as the detectors for H_2O, NH_3, NO and many other chemical vapors [19]-[29], but there is little research on systematic study about improving the surface ratio of MoS_2.

Here, we report the synthesis of the micro-MoS_2 composed of MoS_2 nanosheet with high surface ratio.

Through regulating the concentration of the reactant and the temperature, the morphology and the size of the MoS_2 grain will be different. This work shows that the surface ratio of micro-MoS_2 grains can be improved by regulating reactant concentration and temperature.

2. Experimental

2.1. Preparation of Samples

The $(NH_4)_2MoO_4$, N_2H_4 and S (All purchased from the Sinopharm Chemical Reagent Co., Ltd.) are the reagents used in the experiment, and they are all analytical purity. The reaction vessels (autoclaves) are 25 ml polytetrafluoroethylene liner, which must be wrapped in the stainless hydrothermal reactor. Nine autoclaves were divided into 3 groups (A, B, C). The reaction temperature of and the reactant concentration of group A, B, C are different, the details are shown in **Table 1**.

2.2. Experimental Methods

The deionized water, S, N_2H_4 and $(NH_4)_2MoO_4$ (details shown in **Table 1**) were dispersed in hydrazine hydrate, then the solution was transferred to the 25 ml polytetrafluoroethylene liner, the polytetrafluoroethylene liner was put into stainless steel hydrothermal reactor. After tightening the reactor, it was placed into a calorstat, the temperature of the calorstat was kept at a constant value in 24 h, **Figure 1** shows this process, after that the reactor was naturally cooled to room temperature, then the solutions were filtered, distilled and dried to obtain reaction production.

Table 1. Reactant quantity and temperature of group A, B, C.

Group/T	Reactant				
	NO.	$(NH_4)_2MoO_4$	N_2H_4	S	H_2O
A/180˚C	1	0.75 g	9 ml	0.27 g	6 ml
	2	0.5 g	6 ml	0.18 g	9 ml
	3	0.25 g	3 ml	0.09 g	12 ml
B/200˚C	1	0.75 g	9 ml	0.27 g	6 ml
	2	0.5 g	6 ml	0.18 g	9 ml
	3	0.25 g	3 ml	0.09 g	12 ml
C/220˚C	1	0.75 g	9 ml	0.27 g	6 ml
	2	0.5 g	6 ml	0.18 g	9 ml
	3	0.25 g	3 ml	0.09 g	12 ml

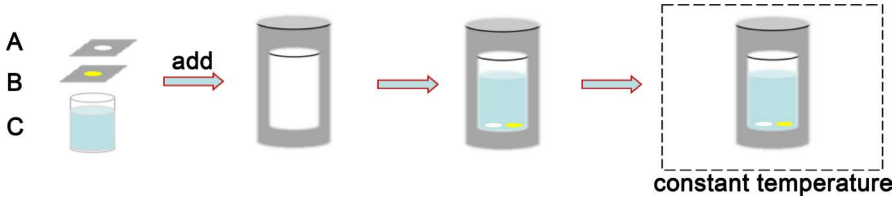

Figure 1. Schematic diagram of processes of the hydrothermal synthesis (A: $(NH_4)_2MoO_4$, B: S, C: N_2H_4 and deionized water).

2.3. Characterization of the Composition, Structure and Morphology of As-Prepared MoS_2/MoO_3 and MoS_2 Samples

Laser confocal Raman spectroscopy (Horiba JobinYvon LabRAM HR800 532 nm 200 - 1100), Crystal structure was analyzed by X-ray diffraction (PANalytical PW3040/60, voltage 40 kV, current 40 mA, Cu Kα radiation (λ = 1.5406), 2θ = 10˚ - 80˚). Morphologies and compositions of the samples were characterized using scanning electron microscopy (SEM, HITACHI S-4800, 5.0 kV).

3. Result and Discussion

Figure 2 shows the Raman spectra of group A, B and C. the picture (1) is the Raman spectra of group A, the picture (2) is the Raman spectra of group B, the picture (3) is the Raman spectra of group C. It can be observed that all groups have three main peaks at 285 cm^{-1}, 823 cm^{-1} and 996 cm^{-1} of α-MoO_3, this match well with the results in previous work [30], but Raman peak intensity of group A (180˚C) is the highest and group C (220˚C) is the lowest no matter how much the reactant concentration is, so temperature is the main fact impacting the hydrothermal synthesis and the higher the temperature, the less MoO_3 come into being. When the temperature rises to 200˚C or 220˚C it will pass 180˚C not immediately, so we can conclude that $(NH_4)_2MoO_4$ will becoming MoO_3 first and then the MoO_3 react with S and N_2H_4 to produce MoS_2 in the condition of group B and C. We can see that the peak intensity of 405 (A1g mode) and 385 (E12g

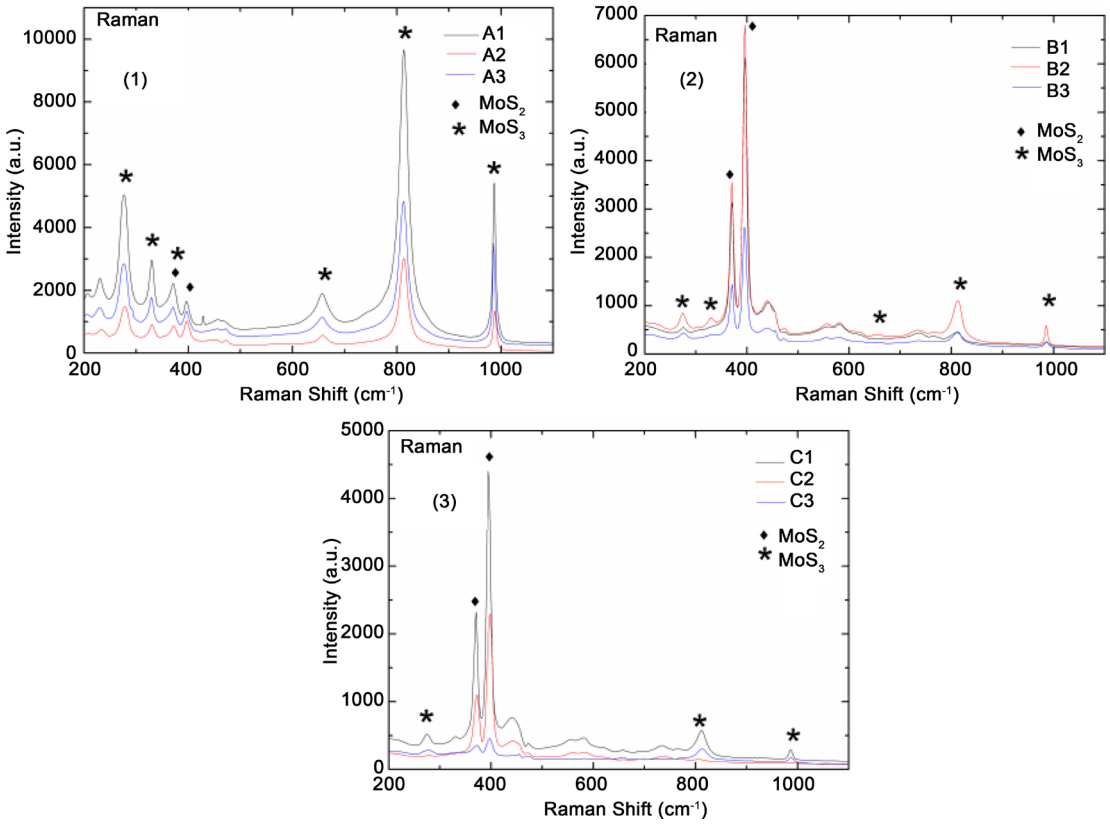

Figure 2. Raman spectra of group A(1), B(2) and C(3).

mode) appear which approved the existence of MoS_2 [31].

Figure 3 shows the XRD patterns of groups A, B, C, the picture (1), (2) and (3) are the XRD patterns of group A, B, C. There are there obvious diffraction peaks at 2˚ of 14.1, 32.9˚, 35.9˚, that corresponding to (0 0 2), (1 0 0) and (1 0 2) planes of MoS_2 in every group, which suggests that MoS_2 is synthesized (JCPDS 75-1539). There are three diffraction peaks at 2˚ of 12.0˚, 12.8˚and 17.6˚, that corresponding to (0 0 1), (0 1 0) and (0 1 1) planes of MoO_3 in group A, which suggests that the MoS_2 synthesized in group A contain MoO_3 (JCPDS 73-1544)

Figure 4 shows the SEM images of groups A, B, C. We can see that every group consists of MoS_2 nanosheet, the MoS_2 nanosheet is about 14 nm thickness, but the size of the nanosheet is different, temperature and concentration impact the morphology of MoS_2, the higher the concentration of reactant the bigger the nanosheet will be produced, the higher the temperature the bigger the nanosheet will be produced. A3 generated microsphere structure and its diameter is 1.215 μm, when the concentration increase from A3 to A2 and A1 the microsphere structure disappeared, so low concentration of reactant is good for generating microsphere structure. From the comparison of A3, B3 and C3 we can see that microsphere structure did not appear at high temperature (200˚C, 220˚C), so high temperature (>200˚C) will restrain the generating of microsphere structure.

Because of van der Waals forces, the nearby MoS_2 nanosheet trend to gather together forming MoS_2 grains. The distance between the nearby MoS_2 nanosheet

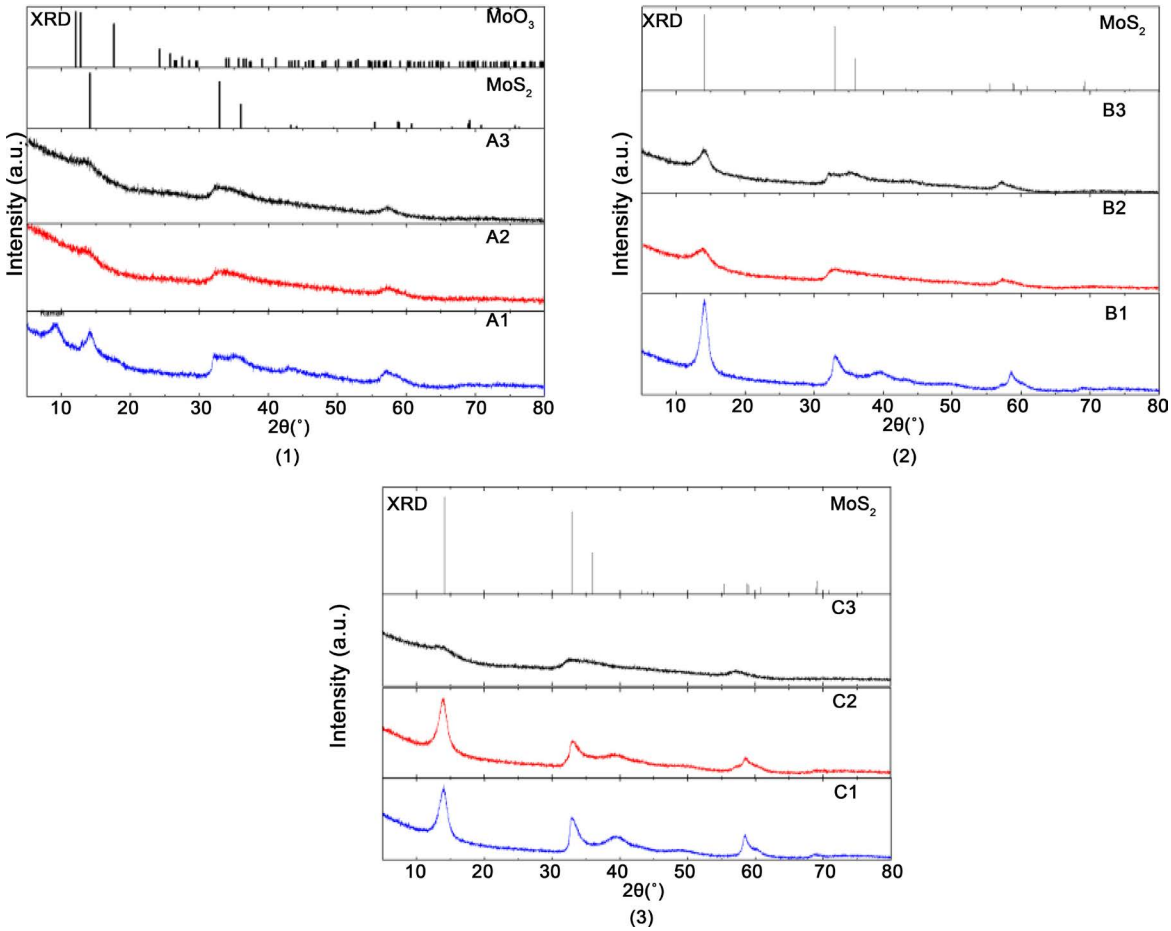

Figure 3. XRD patterns of group A, B and C, typical patterns of MoS_2 and MoO_3 (JCPDS 75-1539, JCPDS 73-1544).

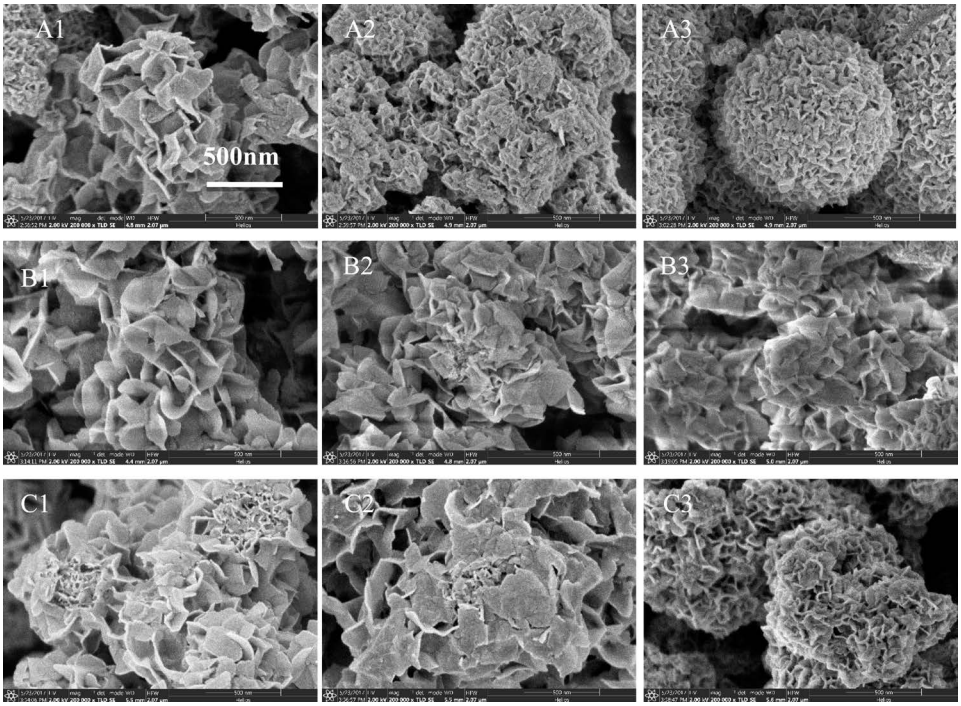

Figure 4. SEM images of group A, B and C (20 K). The rest of figures share the scale in figure A.

will determine the size and amount of nanosheet in a unit of the grain (surface ratio), so the surface of MoS_2 nanosheets will be different in surface ratio. From Figure 4 it can be easily found that when the concentration increase from A3 to A2 and A1 the distance between the nearby MoS_2 nanosheets increasing, when the temperature increase from 180˚C to 200˚C and 220˚C the distance between the nearby MoS_2 nanosheet increasing.

From Figure 4 to get 20 points, in order to get the average distance of the nearby MoS_2 nanosheet as shown in the Table 2**.** To simplify the calculation, it is assumed that all the morphology of each group are sphere and only one surface across the body-center of the sphere as shown in Figure 5, the simplified calculation results show in the Table 2. From the result, it can be seen that when the concentration increase from A3 to A2 and A1 the surface ratio of the nearby MoS_2 nanosheet decrease, when the temperature increase from 180˚C to 200˚C and 220˚C the surface ratio of the nearby MoS_2 nanosheet increasing andA3 has the highest surface ratio 0.0218 nm/nm^2.

On the micro level, the kinetic energy of the molecule is proportional to the temperature. It is obvious that the temperature gradient exist in the reaction vessels, so the kinetic energy of the H_2O molecule are different in the direction of

Table 2. The approximate value of the distance between nearby MoS_2 nanosheet of group A, B, C.

Group/T			
A/180˚C	1	2	3
nm	93	53	39
Surface ratio (nm/nm^2)	0.0091	0.0166	0.0218
B/200˚C	1	2	3
nm	121	112	83
Surface ratio (nm/nm^2)	0.0075	0.0072	0.0114
C/220˚C	1	2	3
nm	102	113	71
Surface ratio (nm/nm^2)	0.0068	0.0071	0.0132

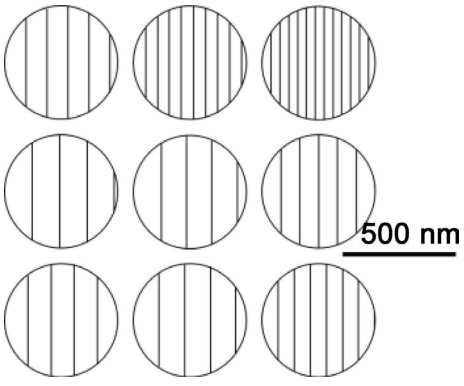

Figure 5. The plan sketch assumed in the calculation of each group.

the temperature gradient, so when temperature increasing, the kinetic energy of the H_2O molecule increase and there will be more H_2O molecule knock the MoS_2 nanosheet, when its impact is bigger than the Van de Waals force, the Van de Waals force cannot to draw the nearby MoS_2 nanosheet to get closer, so the distance of the nearby MoS_2 nanosheet will be far. At the beginning of the reaction, MoS_2 tend to form nanosheet to different direction, when the concentration of reactant is small, the rapid of forming the MoS_2 nanosheet is relatively slow, the Van de Waals force have enough time to draw the nearby MoS_2 nanosheet to get close, so the distance of the nearby MoS_2 nanosheet is small, on the contrary when the concentration of reactant is high, the rapid of forming the MoS_2 nanosheet is relatively fast, before the Van de Waals force drawing the nearby MoS_2 nanosheet to get more close the MoS_2 nanosheet have formed a steady structure that can balance it, so the distance of the nearby MoS_2 nanosheet is far, but as the reaction going on the concentration of reactant will become small, so near the last formed nearby MoS_2 nanosheet their distance will be small, that explained why in the high concentration situation the distance of the nearby MoS_2 nanosheet is inconformity so high concentration of reactant and temperature will increase the distance between the nearby MoS_2 nanosheet and decrease the surface ratio of MoS_2. In other words, low concentration of reactant and temperature will decrease the distance between the nearby MoS_2 nanosheet and increase the surface ratio of MoS_2, which could improve MoS_2 to absorb and storage gases.

4. Conclusion

The micro-MoS_2 grains were synthesized with one-step hydrothermal synthesis. The micro-MoS_2 grains are made of MoS_2 nanosheet. Low concentration of reactant and temperature will be good for forming nanosheet and increase the distance between the nearby MoS_2 nanosheet. Low concentration of reactant and temperature will increase the surface ratio of MoS_2.

Acknowledgements

This work is supported by the National Natural Science Foundation of China (Grant No.51472096), the R&D Program of Ministry of Education of China (No.62501040202). The authors acknowledge the Analytical and Testing Center of Huazhong University of Science and Technology (HUST) for providing Raman measurements. The authors acknowledge the Advanced Manufacturing and Technology Experiment Center of Mechanical College for providing the field emission scanning electron microscope measurements.

References

[1] Mcdonnell, S.J. and Wallace, R.M. (1892) Atomically-Thin Layered Films for Device Applications Based upon 2D TMDC Materials. *Thin Solid Films*, **616**, 482-501. https://doi.org/10.1016/j.tsf.2016.08.068

[2] Hamdi, A., Boussekey, L., Roussel, P., *et al.* (2016) Hydrothermal Preparation of

MoS_2/TiO_2/Si Nanowires Composite with Enhanced Photocatalytic Performance under Visible Light. *Materials & Design*, **109**, 634-643. https://doi.org/10.1016/j.matdes.2016.07.098

[3] Zhang, W., Zhang, P., Su, Z. and Wei, G. (2015) Synthesis and Sensors Application of MoS_2-Based Nanocomposites. *Nanoscale*, **7**, 18. https://doi.org/10.1039/C5NR06121K

[4] Novoselov, K.S., Geim, A.K., Morozov, S.V., Jiang, D., Zhang, Y., Dubonos, S.V., Grigorieva, I.V. and Firsov, A.A. (2004) Electric Field Effect in Atomically Thin Carbon Films. *Science*, **306**, 666-669. https://doi.org/10.1126/science.1102896

[5] Geim, A.K. and Novoselov, K.S. (2009) The Rise of Graphene. *Nature Materials*, **6**, 183-191. https://doi.org/10.1038/nmat1849

[6] Mccann, E. and Koshino, M. (2012) The Electronic Properties of Bilayer Graphene, *Reports on Progress in Physics*, **76**, Article ID: 056503.

[7] Lee, C., Wei, X., Kysar, J.W. and Hone, J. (2008) Strength of Monolayer Graphene Measurement of the Elastic Properties and Intrinsic. *Science*, **321**, 385-388. https://doi.org/10.1126/science.1157996

[8] Tiwari, A. (2015) Graphene-Based Composite Materials. *Dissertations & Theses—Gradworks*, **442**, 282-286.

[9] Balandin, A.A., Ghosh, S., Bao, W., Calizo, I., Teweldebrhan, D., Miao, F. and Lau, C.N. (2008) Superior Thermal Conductivity of Single-Layer Graphene. *Nano Letters*, **8**, 902-907. https://doi.org/10.1021/nl0731872

[10] Ghasemi, F. and Mohajerzadeh, S. (2016) Sequential Solvent Exchange Method for Con-Trolled Exfoliation of MoS_2 Suitable for Phototransistor Fabrication. *ACS Applied Materials & Interfaces*, **8**, 31179-31191.

[11] Yang, T., Cui, Y., Chen, M., *et al.* (2017) Uniform and Vertically Oriented ZnO Nano-Sheets Based on Thin-Layered MoS_2: Synthesis and High-Sensing Ability. *ACS Sustainable Chemistry & Engineering*, **5**, 1332-1338.

[12] Cao, X.H., Shi, Y.M., Shi, W.H., Rui, X.H., Yan, Q.Y., Kong, J. and Zhang, H. (2013) Preparation of MoS_2 Coated Three Dimensional Graphene Networks for High-Performance Anode Material in Lithium-Ion Batteries. *Small*, **9**, 3433-3438. https://doi.org/10.1002/smll.201202697

[13] Tran, M., Banister, D., Bishop, J.D.K. and McCulloch, M.D. (2012) Realizing the Electric-Vehicle Revolution. *Nature Climate Change*, **2**, 328-333. https://doi.org/10.1038/nclimate1429

[14] He, Y.B., Zhou, W., Yildirim, T. and Chen, B.L. (2013) A Series of Metal-Organic Frameworks with High Methane Uptake and an Empirical Equation for Predicting Methane Storage Capacity. *Energy & Environmental Science*, **6**, 2735-2744. https://doi.org/10.1039/c3ee41166d

[15] Gutfleisch, O., Willard, M.A., Bruck, E., Chen, C.H., Sankar, S.G. and Liu, J.P. (2011) Magnetic Materials and Devices for the 21st Century: Stronger, Lighter, and More Energy Efficient. *Advanced Materials*, **23**, 821-842. https://doi.org/10.1002/adma.201002180

[16] Jacobson, M.Z., Colella, W.G. and Golden, D.M. (2005) Cleaning the Air and Improving Health with Hydrogen Fuel-Cell Vehicles. *Science*, **308**, 1901-1905.

[17] Qi, T., Jiang, J.J., Chen, H.C., Wan, H.Z., Miao, L. and Zhang, L. (2013) Synergistic Effect of Fe_3O_4/Reduced Grephene Oxide Nanocomposites for Supercapacitors with Good Cycling Life. *Electrochimica Acta*, **114**, 674-680. https://doi.org/10.1016/j.electacta.2013.10.068

[18] Chen, L.X., Zhu, Y.F., Yang, C.C., *et al.* (2016) A New Strategy to Improve the High-Rate Performance of Hydrogen Storage Alloys with MoS_2, Nanosheets. *Journal of Power Sources*, **333**, 17-23. https://doi.org/10.1016/j.jpowsour.2016.09.148

[19] Baek, D.H. and Kim, J. (2017) MoS_2, Gas Sensor Functionalized by Pd for the Detection of Hydrogen. *Sensors & Actuators B: Chemical*, **250**, 686-691. https://doi.org/10.1016/j.snb.2017.05.028

[20] Mcdonnell, S.J. and Wallace, R.M. (2016) Atomically-Thin Layered Films for Device Applications Based upon 2D TMDC Materials. *Thin Solid Films*, **616**, 482-501.

[21] Yao, Y., Tolentino, L., Yang, Z., Song, X., Zhang, W., Chen, Y. and Wong, C. (2013) High-Concentration Aqueous Dispersions of MoS_2. *Advanced Functional Materials*, **23**, 3577-3583. https://doi.org/10.1002/adfm.201201843

[22] Late, D.J., Huang, Y.-K., Liu, B., Acharya, J., Shirodkar, S.N., Luo, J., Yang, A., Charles, D., Waghmare, U.V., Dravid, V.P. and Rao, C.N.R. (2013) Sensing Behavior of Atomically Thin-Layered MoS2 Transistors. *ACS Nano*, **7**, 4879-4891. https://doi.org/10.1021/nn400026u

[23] Perkins, F.K., Friedman, A.L., Cobas, E., Campbell, P.M., Jernigan, G.G. and Jonker, B.T. (2013) Chemical Vapor Sensing with Monolayer MoS_2. *Nano Letters*, **13**, 668-673. https://doi.org/10.1021/nl3043079

[24] Lee, K., Gatensby, R., Mcevoy, N., Hallam, T. and Duesberg, G.S. (2013) High-Performance Sensors Based on Molybdenum Disulfide Thin Films. *Advanced Materials*, **25**, 6699-6702. https://doi.org/10.1002/adma.201303230

[25] Zhang, S.-L., Choi, H.-H., Yue, H.-Y. and Yang, W.-C. (2014) Controlled Exfoliation of Molybdenum Disulfide for Developing Thin Film Humidity Sensor. *Current Applied Physics*, **14**, 264-268. https://doi.org/10.1016/j.cap.2013.11.031

[26] Liu, K., Feng, J., Kis, A. and Radenovic, A. (2014) Atomically Thin Molybdenum Disulfide Nanopores with High Sensitivity for DNA Translocation. *ACS Nano*, **8**, 2504-2511. https://doi.org/10.1021/nn406102h

[27] Li, H., Yin, Z., He, Q., Li, H., Huang, X., Lu, G., Fam, D.W.H., Tok, A.L.Y., Zhang, Q. and Zhang, H. (2012) Fabrication of Single- and Multilayer MoS_2 Film-Based Filed-Effect Transistors for Sensing NO at Room Temperature. *Small*, **8**, 63-67. https://doi.org/10.1002/smll.201101016

[28] Eda, G., Yamaguchi, H., Voiry, D., Fujita, T., Chen, M. and Chhowalla, M. (2011) Photoluminescence from Chemically Exfoliated MoS_2. *Nano Letters*, **11**, 5111-5116. https://doi.org/10.1021/nl201874w

[29] Zhang, L., Liu, T., Li, T., *et al.* (2017) A Study on Monolayer MoS_2, Doping at the S Site via the First Principle Calculations. *Physica E: Low-Dimensional Systems and Nanostructures*, **94**, 47-52. https://doi.org/10.1016/j.physa.2017.04.173

[30] Silveira, J.V., Batista, J.A., Saraiva, G.D., *et al.* (2010) Temperature Dependent Behavior of Single Walled MoO_3, Nanotubes: A Raman Spectroscopy Study. *Vibrational Spectroscopy*, **54**, 179-183. https://doi.org/10.1016/j.vibspec.2010.10.002

[31] Wang, W., Zeng, X., Wu, S., *et al.* (2017) Effect of Mo Concentration on Shape and Size of Monolayer MoS_2 Crystals by Chemical Vapor Deposition. *Journal of Physics D: Applied Physics*, **50**, Article ID: 395501.